Advances in Industrial and Manufacturing Engineering 3 (2021) 100051

Contents lists available at ScienceDirect

Advances in Industrial and Manufacturing Engineering

journal homepage: www.journals.elsevier.com/advances-in-industrial-and-manufacturing-engineering

Fast, lean-and-agile, multi-parameter multi-trending robust quality screening in a 3D-printed product

George Besseris

Advanced Industrial and Manufacturing Systems, Mechanical Engineering Department, The University of West Attica (Greece) and Kingston University, UK

ARTICLE INFO

Keywords:
3D-product improvement
Robust multifactorial screening/optimization
Fractional factorial designs
Small sample
Data messiness/complexity

ABSTRACT

Additive manufacturing (AM) has revolutionized the local production realization of highly customizable items. However, the high process complexity - inherent to AM operations - renders uncertain the quality performance of the final products. Consequently, there is often a need to assess the unique fabrication capabilities of AM against the reoccurring issues of process instability and end-product inconsistency. Improvement opportunities may be identified by empirically exploring the complex phenomena that regulate the quality performance of the final products. Thus, focused quality-screening and process optimization studies should additionally take into account the special need for speedy, practical and economical experimentation. Robust multi-factorial solvers should predict effect strength by relying on small samples while possibly dealing with non-linear and non-normal trends. We propose a nonparametric modification to the classical Taguchi method in order to enable the generation of rapid and robust screening/optimization predictions for an arbitrary 3D-printing process. The new methodology is elucidated in a recently published dataset that involves the difficult Taguchi screening/optimization application of a fused deposition process. We compare differences in the predicted effect-strength magnitudes between the two approaches. We comment on the practical advantages that the new technique might offer over the traditional Taguchi-based improvement analysis. The emphasis is placed on the 'assumption-free' aspect, which is embodied in the new solver. It is shown that the proposed tool is agile. It could also reliably support a customized 3D-printing process by offering robust and faster quality improvement predictions.

1. Introduction

Additive manufacturing ushers in a new epoch in industrial operations by placing a great emphasis on innovative custom-based production tactics (Redwood et al., 2017; Lipson and Kurman, 2013; Chua and Leong, 2017; Thompson et al., 2016). Additive manufacturing utterly diverges in philosophy from the traditional 'subtractive-and-formative' production mentality via the promotion of the revolutionary idea of "bottom-up creation" (Tofail et al., 2018; Satish Prakash et al., 2018). The technological strategy of 3D-printing is at the core of additive manufacturing because it provides the technical catalyst for the direct conversion of computer-aided designs (CAD) to rapidly prototyped and mass-personalized objects (Gibson et al., 2015). It is 3D-printing that reifies a digital model, 'layer-by-layer', to a physical end-product. An increasing number of contemporary literature reviews supports the potential benefits of engaging additive manufacturing in popular product-making. Primary working materials may include: composites (metal alloys, ceramics, polymers and concrete) (Ngo et al., 2018; Wang et al., 2017), micro- and nano-multidirectional composites (Quan et al., 2015; Farahani and Dube, 2018), polymer-fibers (Parandoush and Lin, 2017), novel materials (Lee et al., 2017), biomaterials (Bose et al., 2018), non-assembly mechanisms (Cuellar et al., 2018), part-decomposition designs (Oh et al., 2018), functionally-graded materials (Loh et al., 2018), 3D-printed polymers (Dizon et al., 2018), multi-material structures (Bandyopadhyay and Heer, 2018), medical applications with bio-printing (Yan et al., 2018; Kacarevic et al., 2018), high-precision therapeutics (Trivedi et al., 2018), metals (Francois et al., 2017) and advanced smart materials (Chang et al., 2018). It is anticipated that it could be extended in the near future to cover broader areas of specialization.

The opportunities for disruptive innovation through the adoption of additive manufacturing over traditional production methods have been greatly reviewed (Eyers and Potter, 2017; Attaran, 2017; Petrick and Simpson, 2013; Gao et al., 2015). In brief, they are associated to freedom of design, flexibility, scalability, on-demand manufacturability as well as mass customization. The same features unequivocally comprise the crux of the popular operational strategy known as agile manufacturing (Le, 2018; Potdar et al., 2017). Moreover, the 3D-printing fabrication

E-mail address: besseris@uniwa.gr.

https://doi.org/10.1016/j.aime.2021.100051
Received 23 September 2020; Received in revised form 21 April 2021; Accepted 28 April 2021

mentality aligns with the fast, cost-driven, and lean engineering principles. Lean production promotes zero-waste operations and just-in-time process scheduling (George et al., 2004; Bhamu and Sangwan, 2014). By instilling simultaneously agile and lean competencies in manufacturing, it elevates product development capabilities to the coveted 'leagile' status (Virmani et al., 2018). Creative thinking, which is supported by quick-and-economical experimentation, catalyzes the discovery pathway toward resilient process and products; it underscores quick response to customer needs and market changes (Alves et al., 2012). To achieve dominance over decentralized modular forming, which is governed by material and geometric complexities, additive manufacturing must leverage the aesthetic and functional quality issues that might tarnish the end products (Tofail et al., 2018; Eyers and Potter, 2017; Attaran, 2017). Moreover, quality leadership should assist in accelerating the product development progress, by boosting the rapid-prototype verification, and by validating the production efficiency cycle. This might be managed via the breakthrough tactics and methods of the lean six sigma initiative (George et al., 2004). In general, it is admitted that the confluence of lean six sigma tools and agile engineering methods spur competitive advantage (Kovach et al., 2005). This synergistic effect should enhance the quality of the 3D-printed fabrication results, because, as mentioned above, the additive manufacturing technology naturally fosters the leagile mentality as its core technical archetype. Furthermore, the same archetype spawns a score of eco-innovation drivers that legitimizes additive manufacturing as the designated sustainable production mediator (Ghobadian et al., 2020; Afshari et al., 2020; Mellor et al., 2014).

The 3D-printing technology applications have seen an increase of almost 50% in highly critical industries, such as in the automotive, medical, aerospace and military sectors (Kim et al., 2018). Thus, advanced quality performance becomes imperative for this novel technology to flourish. Unfortunately, quality control problems have been recorded to be unique, complicated and of great variety (Wu and Chen, 2018). Mainly, they are associated with the preciseness, repeatability, reproducibility, and reliability of their end-product key-characteristics. Specifically, parameter variations in laser power, powder composition and material-layer thickness may tweak the melt-flow propensities, which in turn perturb the material porosity, microstructure, surface roughness as well as the geometric structure. Similarly, the wire-arc (non-powder) additive fabrication process may be plagued by high residual stresses, unstable microstructures, solute segregation, and multi-phase solidification (Cunningham et al., 2018). A non-uniform thermal profile may exacerbate the end-product anisotropy and heterogeneity. Consequently, an enduring low-quality performance clearly drives the high cost of production, which in additive manufacturing constitutes one of its pivotal barriers that hamper the progress of this promising technology (Thomas-Seale et al., 2018).

The challenges of designing quality into the additive manufacturing processes have been recently delineated (Colosimo et al., 2018). The ensuing opportunities have been identified to resolving three distinct types of complexities, in connection with: 1) the product geometry, 2) the process optimization, and 3) the product data collection. Complexity awareness is vital in many-component systems that are successively part of other larger systems. For example, a biological cell or a central processing unit are complex systems that belong to even larger complex systems, such as living organs or electronic devices, respectively (Carlson and Doyle, 2002). Nevertheless, in additive manufacturing "the complexity is for free" (Fera et al., 2018). This is because the cost of complexity in highly adaptable processes is always minimized (Orr, 2000). The minimization of the cost of complexity is an evolutionary robust result (Welch and Waxman, 2003), which makes explaining novel 3D-printing phenomena scientifically intriguing. However, complexity and quality conspicuously appear to share a common fate. "Quality is free, but not a gift" was proclaimed by the quality guru Crosby (1979). Surely, we do not overlook the assertion in production economics that was made by the famed quality philosopher Genichi Taguchi: "Cost is more important than quality, but quality is the best way to reduce cost". We conclude, then, that the costs of quality and complexity are minimized when product/process characteristics are optimized. However, process complexity is also an emerging challenge for the quality management field itself and thus it tempts extra forethought (Kuhn et al., 2018). Contemporary quality philosophy has evolved to *lean six sigma* - a process-improvement data-driven initiative – to reduce companywide costs (George et al., 2004). Quality improvement luminary Shigeo Shingo has advocated the prioritization of improving process outcomes in an increasing order of importance: "easier, better, faster and cheaper". It heavily relies on 'cause-and-effect' empirical modelling and techniques. On the other hand, empirical modelling has grown into offering a competitive edge in discovering and optimizing rapid-prototype processes (Garg et al., 2014). Quantification of uncertainty is an essential task when investigating any 'cause-and-effect' relationships (Briggs, 2016). Furthermore, uncertainty and robustness are innately intertwined in theoretical terms (Hoaglin et al., 2000; Huber and Ronchetti, 2009) and greatly influenced by complexity (Carlson and Doyle, 2002). Then, ensuring model robustness may be anticipated as a staple in advanced additive manufacturing (Gholaminezhad et al., 2016).

In the lean-six-sigma strategy, robust design is a standard tactic – established on empirical modelling (George et al., 2004). It is in common practice in additive manufacturing (Wu and Chen, 2018). Robust design comprises of a statistically engineered toolset that is founded on Design of Experiments (DOE) (Box et al., 2005; Goh, 1992). Particularly popular in additive manufacturing is Taguchi's 'design-and-analysis' technique (Taguchi et al., 2000, 2004). The experimental design phase is devoted to planning a minimal number of trials by suitably selecting those combinations of the studied effects that maximize information generation. The settings of the examined controlling factors are programmed in terms of trial recipes through fractional factorial designs (FFDs). The preferred FFD schemes that have been adopted in the Taguchi methods are a series of orthogonal arrays (OAs) that may accommodate: 1) linear, 2) non-linear or even 3) a mix of linear and non-linear dependencies (Taguchi et al., 2004). In the analysis phase, a single-step double--optimization effort is attempted to 1) screen out weak effects (shorten the initial list of examined factors) and 2) locate those settings of the strong effects that optimize the studied product/process response(s). Taguchi methods are especially attractive in fast product realization, because they aid in accelerating the product development cycle while minimizing product failure, product costs, line-machinery engagement, trial costs and project execution time. Indicatively, Taguchi methods have been implemented in additive manufacturing in interlayer bonding improvement of extrusion components (Fitzharris et al., 2018), fused deposition in the fabrication of lattice structures (Dong et al., 2018), minimization of warpage in sintered polymer parts (Dastjerdi et al., 2017), and dimension and tolerance control of fused deposition (Mahmooda et al., 2018). Nevertheless, there are several intricacies that are associated with the usage of Taguchi methods in 3D-printing that may impede their broader applicability to any optimization problem. To render robust the behavior of a characteristic response, Taguchi methods require replicated datasets in order to evaluate the repeatability/reproducibility status of predictions. This necessity - the sufficiently large number of replicates - might hamper the Taguchi-based optimization approach to become effective in wider rapid-prototyping applications (Wu and Chen, 2018). Moreover, the recommended measure for capturing the replicate variation is obtained from the Taguchi-defined signal-to-noise ratio (SNR) expressions (Taguchi et al., 2004; Ganeshan et al., 2001). Replicated datasets that participate in SNR estimations are assumed to follow normality. Nevertheless, normality is a condition that is not warranted in 3D-printing phenomena. Consequently, this dubiety could raise specific issues with respect to the general applicability of the original Taguchi-type SNR data analysis (Schippers, 1998; Box, 1988; Maghsoodloo et al., 2004; Pignatiello and Ramberg, 1992). Conducive to the complexity of printable materials, ordinary multi-parameter optimization treatments, such as those resulting from the analysis of variance

(ANOVA) and the general linear regression modelling (GLM) may not always be valid.

A primary utilization of DOE is to uncover those strong input parameters that influence the total quality performance under process uncertainties from an economic standpoint (Natarajan, 1993; Murthy and Ravi Kumar, 2000; Fundin et al., 2018; Tari and Sabater, 2009). Meanwhile, complexity might induce experimental uncertainty to beget "messy" datasets (Milliken and Johnson, 2004). Messy data are peculiar groups of observations, the statistical distributions of which are hard to fingerprint with ordinary means. Consequently, it might be futile to employ regular multi-factorial treatments such as ANOVA and GLM to make predictions. This stems from the fact that the clarity of the outcome interpretations is susceptible to several critical assumptions. For ANOVA, such assumptions are 1) the randomness of errors, 2) the independence of errors, 3) the normality, and 4) the homogeneity of variance. For GLM, it implicates the residual analysis, which must confirm the validity of the following assumptions: 1) normality, 2) homoscedasticity, 3) independence and 4) autocorrelation. It becomes apparent now that in the case that we ought to confront messy data, the expected performance of an ordinary multifactorial tool would be doubtful to be judged as either accurate or 'leagile'.

An additional - less obvious – assumption is an inherent limitation that instructs against conducting protracted trial replications (Wu and Chen, 2018). The extent of replication is analogous to what is only deemed practical, expedient and economical in each specific study. However, a minimal replication effort may not be even adequate to discern if data normality holds or not. On the other hand, normality is a strict requirement for the Taguchi-type SNR estimations to be valid. Therefore, caution should be exercised in deciding to implement the SNR estimator for data reduction with the provisos: 1) few replicates, and 2) observations prone to a "messy" manifestation. If the statistical distribution remains undetermined, opting to a classical Taguchi-based factorial analysis might endanger the prediction reliability (Silver, 2015). A possible remedy would be to resort to basic nonparametric theory (Hettmansperger and McKean, 2010; Hollander et al., 2013). This might be justifiable since it has been suggested that order statistics could potentially harmonize the information extraction process from small-data samples of unresolved statistical nature (Siebert and Siebert, 2017; Pett, 2015). Moreover, nonparametrics have been found to be more reliable data analyzers for highly complex processes - such as regarding biological systems - than other common solvers (Ludbrook and Dudley, 1998).

The purpose of this work is to propose a statistical multi-factorial screening/optimization method for the general 3D-printing paradigm. It considers the realistic circumstances that are to be encountered during the fabrication process: i) data messiness owing to innate process complexity, ii) necessity for small sampling, iii) mixed-type effects (a blend of linear and non-linear factors), iv) need for robust predictions, v) mixed-type balanced/unbalanced factor-settings and vi) fast data-processing cycle - by eliminating several core assumptions of alternative mainstream tools. The technique deploys the rank-sum estimator (Wilcoxon, 1945; Mann and Whitney, 1947) in order to non-parametrically summarize 'micro-population' tendencies, which are derived from minimally replicated OA-datasets. Messy data analysis is ensued according to the 'nonreplicated' framework (Milliken and Johnson, 1989). A rudimentary version of the proposed profiler has already been examined only for two trivial setups: 1) on a complex filtration process with linear effects (Besseris, 2013), and 2) in biomedical diagnostics with non-linear effects (Besseris, 2014). The new 'combo-optimizer' interchangeably utilizes Wilcoxon-Mann-Whitney statistics (Wilcoxon, 1945; Mann and Whitney, 1947) and Kruskal-Wallis nonparametrics (Kruskal and Wallis, 1952) to simultaneously profile '*constant-free and distribution-free*', linear and nonlinear, 3D-printing related effects. As a matter of convenience, timeliness and assimilation in utilizing the new technique, we re-examine a very recently published dataset, which was collected for the process optimization of a fused deposition for lattice structures (Dong et al., 2018).

2. Methodology

2.1. Basic assumptions and limitations

The multi-factorial screening/optimization methodology is to be employed to any 3D-printing product/process improvement project. Fractionalized trial plans are programmed by implementing general FFDs (Box et al., 2005) or Taguchi-type OAs (Taguchi et al., 2004). The approach accommodates at least a primitive trial replication tactic via a mere duplication of the prescribed OA-recipes. However, adding a third round of replicates is surely advisable because it could also offer a basal view with regards to data repeatability concerns. It is an economic scheme that maintains the trial volume as low as possible whereas it accelerates the overall project cycle. We define the trial replication number as R. Since improving 3D-printing processes arguably do not favor long repetitive DOE plans (Kim et al., 2018), then, the R value should be generally expected to be small. In a Taguchi-type OA, L_N, N is defined as the number of the prescribed factorial recipes that ought to be executed. In the proposed approach, there are no conditions to be imposed on the structure of the OA scheme with respect to: 1) the number of controlling factor settings, 2) the mix of numbers of settings among different factors, and 3) the balance among factor settings. The first point indicates that the proposed analysis is suitable regardless to probing linear (two-setting) or nonlinear (three-setting or higher) effects. The second point instructs that multifarious linear and non-linear effects may be synchronously studied. The third point removes any restriction on the uniformity of the setting size within a particular effect; it makes an impending unbalanced factorial analysis more versatile and agile.

The robust optimization/screening of product characteristics should be apt to compensate for insidious statistical deviations in the collected datasets. The 3D-printing mechanics of customized items often foster intricate behavior. Non-normality, heteroscedasticity, and the presence of data outliers/extremities may not be extrinsic to such phenomena. We may compound on the previous considerations two other fair yet conflicting speculations. One relates to the contingency of multiple or intermixed statistical distributions. The other case regards to the possibility for an undetermined statistical distribution at all. Either situation may be exacerbated by the smallness of the dataset. Once present, such conditions augment the impact of 'messiness' in the undergoing DOE analysis (Milliken and Johnson, 2004). Nevertheless, a robust multifactorial profiler/optimizer should be capable to translate messy data. It is convenient and agile to propose a distribution-free approach inasmuch as it eliminates the intermediate step of searching for a specific parametric distribution model (Hettmansperger and McKean, 2010; Hollander et al., 2013). In spite of 3D-printing (DOE) studies being linked with small samples and unusual data distributions, a multifactorial solver should also withstand the breakdown of its much-desired robustness capability (Siebert and Siebert, 2017; Pett, 2015). For complex systems, permutation statistics are superior to ordinary t-statistics (Ludbrook and Dudley, 1998). In the formulation that follows we employ classical Wilcoxon (1945) ranking operations to de-parametrize the collected replicate samples. We accumulate the replication effect by viewing a group of replicates as 'micro-populations' - as it was expounded by the Mann and Whitney theory (Mann and Whitney, 1947). This mentality widens the usage scope of the replicate sample as opposed to contrasting merely for sample central tendencies.

2.2. Pre-screening multifactorial DOE datasets

Prior to commencing the effect-profiling procedure, the OA-generated datasets should undergo a pre-processing stage to reveal any disparities from normal statistics. This is performed to determine whether or not it is justifiable to apply the proposed methodology. Before computing the effect strengths, it is instructive to explore the stability

level of the data-reduction process. Therefore, the first step is to prepare a probability plot that represents the data tendencies of the pooled observations. Its 95%-confidence-interval performance should also be displayed. Similarly, the respective probability plots for each examined factor should be prepared whereas the datasets for different settings are portrayed separately. Detecting any departure from normality, in any of the probability plots, may also be facilitated by combining information from a visual inspection, as well as from the fitting performance of the dataset according to the Anderson-Darling test. If there is a strong evidence of departure from normality, the degree of asymmetry in the data spread may be robustly refined by using boxplots.

To probe the level of the dataset repeatability, it is useful to examine the replicate partial correlations using linear regression (GLM modelling). The classical main effects plot for the data means and the classical SNR-measure effects plot may be prepared to provide additional insights. The required data analysis, which is described in this sub-section, is performed using the statistical software package MINITAB v.18.

2.3. Multi-factorial screening/optimization

We examine the influence of **K** controlling factors which are symbolized as: $\boldsymbol{X_1}, \boldsymbol{X_2} \ldots, \boldsymbol{X_K}$. We assume an arbitrary OA which is denoted as: L_N (s_1^{k1}, s_2^{k2}, …, s_c^{kc}) with mixed factor settings $\{s_i \in [2, 3, 4, \ldots] \; \forall \; i = 1,2,..,c\}$. For the N total recipes, the settings for each controlling factor are: x_{1j}, x_{2j}, …, x_{Kj} ($j = 1, 2 \ldots N$). The examined 3D-printing characteristic is arbitrarily denoted as **Y**. A set of R replicated responses will be defined as: $y_{1i}, y_{2i} \ldots y_{Ni} \; \forall \; i = 1, 2, \ldots, R$. The layout of the input-output relationship between the parametrized recipes and the associated response is generically tabulated in Fig. 1. Based on the direction of the optimization goal, a characteristic is usually categorized according to the three general types: 1) maximization, 2) minimization, or 3) minimization of its departure from a target value (Gholaminezhad et al., 2016). By convention, we assign the lowest ranks to the observations that lead toward the optimal direction with respect to the predefined goal (Besseris, 2013, 2014). Next, we rank order all replicated observations by a single roll-out across all replicates. The transformed replicates, $\{r_k\}$, are now identified by the reforming index k: $k = i + N\bullet(j\text{-}1) \; \forall \; 1 \le i \le N$, and $1 \le j \le R$. Therefore, the transformation reduces the initial dimensionality of the replicate matrix:

$$y_{ij} \rightarrow r_k \tag{1}$$

For any given ith recipe, the Wilcoxon rank-sum, $\{rs_i\}$, $\forall \; 1 \le i \le N$ becomes a sample estimator to be checked for parity with respect to the other recipes:

$$rs_i = \sum_{j=1}^{R} r_{i+N\times(j-1)} \tag{2}$$

Consequently, the initial layout (Fig. 1) is now compressed and simplified as shown in Fig. 2. It has been converted to a 'nonreplicated' and saturated form (Milliken and Johnson, 1989).

Factorial recipes *Replicated response*

$$\begin{pmatrix} x_{11} & x_{12} & \cdots & x_{1K} \\ x_{21} & x_{22} & \cdots & x_{2K} \\ \vdots & \vdots & \cdots & \vdots \\ x_{N1} & x_{N2} & \cdots & x_{NK} \end{pmatrix} \left(\begin{bmatrix} y_{11} \\ y_{21} \\ \vdots \\ y_{N1} \end{bmatrix} \begin{bmatrix} y_{12} \\ y_{22} \\ \vdots \\ y_{N2} \end{bmatrix} \cdots \begin{bmatrix} y_{1R} \\ y_{2R} \\ \vdots \\ y_{NR} \end{bmatrix} \right)$$

Fig. 1. General mixed-type orthogonal array scheme and the R-replicated response layout.

$$\begin{pmatrix} x_{11} & x_{12} & \cdots & x_{1K} \\ x_{21} & x_{22} & \cdots & x_{2K} \\ \vdots & \vdots & \cdots & \vdots \\ x_{N1} & x_{N2} & \cdots & x_{NK} \end{pmatrix} \left(\begin{bmatrix} rs_1 \\ rs_2 \\ \vdots \\ rs_N \end{bmatrix} \right)$$

Fig. 2. Rank-sum transformed OA-based observations to a single compounded response.

To examine the influence for each effect, the nonreplicated-saturated OA arrangement of Fig. 2 undergoes a specialized 'messy data' analysis (Milliken and Johnson, 1989). However, the full utilization of the OA structure by the investigated effects allows no additional degrees of freedom to directly estimate the residual error. Thus, a combination of two (linear and nonlinear) surrogate profilers (Besseris, 2013, 2014) will be employed to statistically retrieve: 1) the effect potencies and 2) the uncertainty parities (across different factor settings). The generic rank-sum vector $\{sr_i\}$ of Fig. 2 should be re-indexed to expose the K-effect dependencies in the formalism that follows. Thus, it becomes $\{ sr_{i_1,i_2,\ldots,i_K} \}$ which now it may be fitted to a generalized surrogate model (Besseris, 2013, 2014) - regardless to blending linear and non-linear effect contributions:

$$sr_{i_1,i_2,\ldots,i_K} = M + \sum_{j=1}^{K} D_{i_j} + \varepsilon_{i_1,i_2,\ldots,i_K} \tag{3}$$

The grand median, M, has been defined as:

$$M = med(\{sr_{i_1,i_2,\ldots,i_K}\}) \quad \text{for all} \quad i_1, i_2, .., i_K \tag{4}$$

For the indices (factor levels) $i_1, i_2, \ldots, i_K$, it holds that: $i_j \in [1, 2, 3, \ldots] \; \forall \; 1 \le j \le K$.

The term, $\varepsilon_{i_1,i_2,\ldots,i_K}$, accounts for the experimental uncertainty in a particular factorial recipe. We also need to define the medians for each factor setting, M_{i_l}:

$$\{ \; M_{i_l} = Med(\{LT_{i_1,i_2,\ldots i_l,\ldots,i_K}\}) \quad \forall \; 1 \le l \le K \; \exists \; i_l \in [1, 2, 3, \ldots] \; \}$$
$$\text{for all} \quad i_1, i_2, \ldots, i_{l-1}, i_{l+1} \ldots, i_K \tag{5}$$

From equations (4) and (5), we define the partial median, D_{i_l}, i.e. its difference of the setting median from the grand median:

$$\{ \; D_{i_l} = M_{i_l} - M \; \forall \; 1 \le l \le K \; \exists \; i_l \in [1, 2, 3, \ldots] \; \} \tag{6}$$

To check uncertainty parities within effects, we form the l-effect error vector, $\{rs'_{i_1,i_2,\ldots i_l,\ldots i_m}\}$:

$$rs'_{i_1,i_2,\ldots i_l,\ldots i_K} = M + \varepsilon_{i_1,i_2,\ldots i_l,\ldots i_K} \text{ for all } i_l \text{ and } 1 \le l \le K \tag{7}$$

The rank-ordered error vector becomes:

$$rs'_{i_1,i_2,\ldots i_l,\ldots i_K} \rightarrow r'_{i_1,i_2,\ldots i_l,\ldots i_K} \text{ for all } i_l \text{ and } 1 \le l \le K \tag{8}$$

At this phase, there are two scenarios that should be considered; one or more effects are: 1) linear and/or 2) non-linear.

A) Testing error parity for linear effects: If some effects have been designed to be studied at two settings only, then the minimum rank-sum of rse_{i_l} is formed according to the Wilcoxon rank-sum test (Wilcoxon, 1945; Besseris, 2013):

$$TE_l = \min_{rse_{i_l}} \left\{ \; rse_{i_l} = \sum_{i_j \ne l} r'_{i_1,i_2,\ldots i_l,\ldots i_K} \quad i_l \in [1, 2] \; \right\}$$
$$\text{for all} \quad i_1, i_2, \ldots, i_{l-1}, i_{l+1} \ldots, i_K \tag{9}$$

The minimum rank-sum, TE_l, is translated against the Wilcoxon-Mann-Whitney (Wilcoxon, 1945; Mann and Whitney, 1947) reference law. Exact p-values are obtained using the Mann-Whitney test from the software package MINITAB® (v18.0).

B) Testing error parity for nonlinear effects: If some effects have been designed to be studied at three or more settings, then the Kruskal-Wallis test (Kruskal and Wallis, 1952) is applied to the rank-ordered error vector, $r'_{i_1,i_2,\ldots i_l,\ldots i_K}$, and it will be (Tari and Sabater, 2009):

$$He_l = \left[\frac{12}{N(N+1)}\sum_{i_l}\frac{Re_{i_l}{}^2}{n_{i_l}}\right] - 3(N+1) \quad \forall\, i_l \in [1,\ 2,\ 3,\ \ldots] \tag{10}$$

with

$$\sum_{i_l} n_{i_l} = N \quad \forall\, 1 \le l \le K\ \exists\, i_l \in [1,\ 2,\ 3,\ \ldots] \tag{11}$$

and

$$\left\{\ Re_{i_l} = \sum_{i_l} r'_{i_1,i_2,\ldots i_l,\ldots,i_K} \quad \forall\, 1 \le l \le K\ \exists\, i_l \in [1,\ 2,\ 3,\ \ldots]\ \right\}$$
$$\text{for all}\quad i_1, i_2, \ldots, i_{l-1}, i_{l+1} \ldots, i_K \tag{12}$$

The parity of errors for each effect individually is inferred from the exact p-value that corresponds to the estimation of He_l; it is also obtained from the software package MINITAB® (v18.0). Similarly, we prepare the rank sums for the surrogate effects, $rs'_{i_1,i_2,\ldots i_l,\ldots i_K}$:

$$rs'_{i_1,i_2,\ldots i_l,\ldots i_K} = M + D_{i_l} + \varepsilon_{i_1,i_2,\ldots i_l,\ldots i_K} \text{ for all } i_l \text{ and } 1 \le l \le K \tag{13}$$

Upon rank-ordering, we get:

$$rs'_{i_1,i_2,\ldots i_l,\ldots i_K} \rightarrow r_{i_1,i_2,\ldots i_l,\ldots i_K} \text{ for all } i_l \text{ and } 1 \le l \le K \tag{14}$$

At this phase, there are also two scenarios that should be considered; one or more effects are: 1) linear and/or 2) non-linear.

A) Testing significance for linear effects: If some effects have been designed to be studied at two settings only, then the minimum rank-sum of rs_{i_l} is formed according to the Wilcoxon rank-sum test (Wilcoxon, 1945; Besseris, 2013):

$$T_l = \min_{rs_{i_l}}\left\{\ rs_{i_l} = \sum_{i_j \ne l} r_{i_1,i_2,\ldots i_l,\ldots i_K} \quad i_l \in [1,\ 2]\ \right\} \text{ for all } i_1, i_2, \ldots, i_{l-1}, i_{l+1} \ldots, i_K \tag{15}$$

The minimum rank-sum for each effect, T_l, is translated against the Wilcoxon-Mann-Whitney (Wilcoxon, 1945; Mann and Whitney, 1947) reference law. Exact p-values are obtained using the Mann-Whitney test from the software package MINITAB® (v18.0).

B) Testing significance for nonlinear effects: If some effects have been designed to be studied at three or more settings, then the Kruskal-Wallis test (Kruskal and Wallis, 1952) is applied to the rank-ordered effect vector, $r_{i_1,i_2,\ldots i_l,\ldots i_K}$, and it will be (Besseris, 2014):

$$H_l = \left[\frac{12}{N(N+1)}\sum_{i_l}\frac{R_{i_l}^2}{n_{i_l}}\right] - 3(N+1) \quad \forall\, i_l \in [1,\ 2,\ 3,\ \ldots] \tag{16}$$

with

$$\sum_{i_l} n_{i_l} = N \quad \forall\, 1 \le l \le K\ \exists\, i_l \in [1,\ 2,\ 3,\ \ldots] \tag{17}$$

and

$$\left\{\ R_{i_l} = \sum_{i_l} r_{i_1,i_2,\ldots i_l,\ldots i_K} \quad \forall\, 1 \le l \le K\ \exists\, i_l \in [1,\ 2,\ 3,\ \ldots]\ \right\}$$
$$\text{for all}\quad i_1, i_2, \ldots, i_{l-1}, i_{l+1} \ldots, i_K \tag{18}$$

The statistical significance of each individual effect is inferred from the exact p-value that corresponds to the estimation of H_l; it is also obtained from the software package MINITAB® (v18.0).

2.4. The illustrated case study

To elucidate the necessity for a 'deeper' multifactorial analysis, a state-of-the-art case study is re-examined which enmeshes several opportunities for hidden complexity in a novel 3D-printing process. We selected the Taguchi-type screening/optimization modelling of a fused deposition for the fabrication of lattice structures (Dong et al., 2018). It is an intriguing paradigm because it mingles the uncertainty in the propensities of a crucial cellular material (acrylonitrile butadiene styrene) with the complexity in the tested lattice geometries. Consequently, the intricate (end-product) mechanical properties cannot be reliably predicted from an extant deterministic theory. Furthermore, non-normality in the governing mechanisms of production may not be rejected. Hence, the dual (synchronous) 'screening-and-optimization' task should be addressed also using a robust profiler.

The available published dataset was voluminous. Besides a set of four specific 3D-printing parameters, the study probed the influence of several design parameters, which were associated with two examined geometry groups. To scrutinize the robustness level of the final solution and the optimal prediction of the 3D-printing response, we demonstrate our methodology for the 'inclined' geometry case which was set at an angle of 60° and for a strut diameter of 4 mm (Dong et al., 2018). To summarize the experimental logistics, the investigated 3D-printing factors were: 1) the nozzle temperature (A), 2) the print speed (B), 3) the fan speed (C), and 4) the layer height (D). Three of the 3D-printing factors (A, B and C) were simultaneously tested for non-linearity, too. Accordingly, factors A and B were profiled on four settings while factor C was profiled on three settings. Factors A, B and D were in balanced form across all recipes. However, factor C was organized in an unbalanced arrangement; the first setting frequented the experimental recipes twice as many times as the remaining two settings. The output response from the trials was the range of thickness (dt) of the tested strut diameter, which was expressed in mm. The Taguchi-type L_{16} ($4^2 \times 3^1 \times 2^1$) OA-generated output was repeated three times. The failure method for 'max deviation' was chosen (Dong et al., 2018). The coded OA scheme and the corresponding response entries have been listed in Table 1 for ease of reference.

3. Results

3.1. Data pre-screening

The first step is to screen all the thickness-range (dt) observations (Table 1) in a probability plot. In Fig. 3A, we notice that the data do not spread evenly under the normal distribution assumption. A noticeable

Table 1
The fused deposition OA-dataset for the fabrication of lattice structures (Dong et al., 2018).

Run #	A	B	C	D	dt1	dt2	dt3
1	1	1	1	1	0.52	0.47	0.22
2	1	2	2	2	0.15	0.13	0.11
3	1	3	3	2	0.18	0.15	0.09
4	1	4	1	1	0.47	0.30	0.60
5	2	1	3	1	0.12	0.15	0.09
6	2	2	1	2	0.34	0.38	0.30
7	2	3	1	2	0.27	0.37	0.32
8	2	4	2	1	0.17	0.17	0.18
9	3	1	1	2	0.32	0.26	0.35
10	3	2	3	1	0.10	0.13	0.12
11	3	3	2	1	0.14	0.15	0.18
12	3	4	1	2	0.45	0.32	0.30
13	4	1	2	2	0.04	0.06	0.07
14	4	2	1	1	0.10	0.13	0.12
15	4	3	1	1	0.18	0.23	0.15
16	4	4	3	2	0.14	0.16	0.17

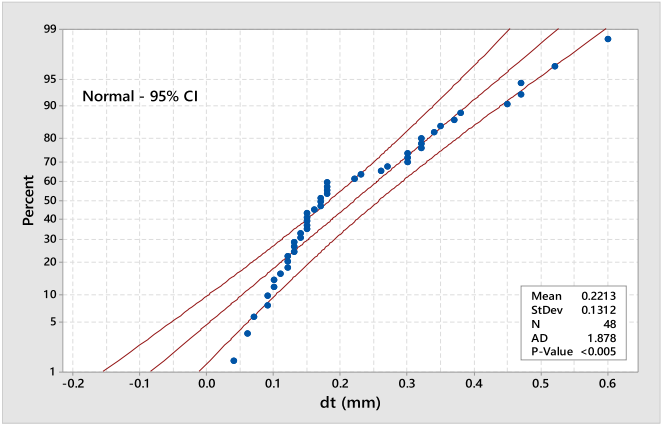

A.

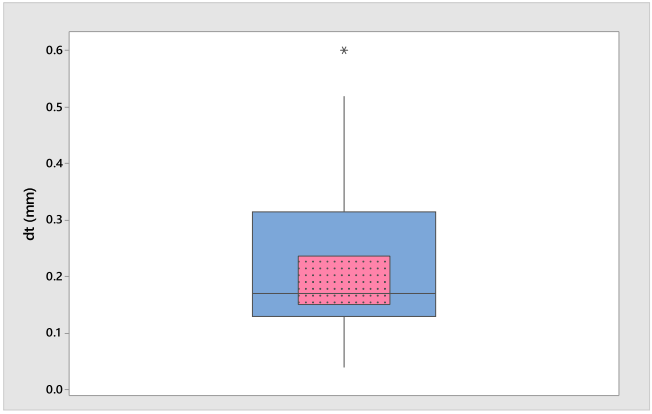

B.

Fig. 3. The dt dataset (Table 1): Normal probability plot with 95% confidence interval (A), and boxplot (B).

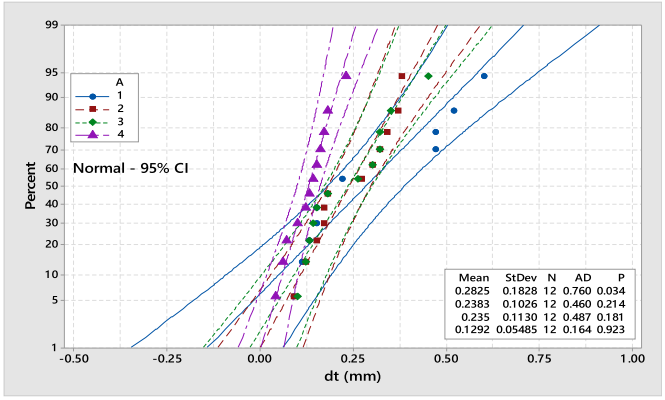

A.

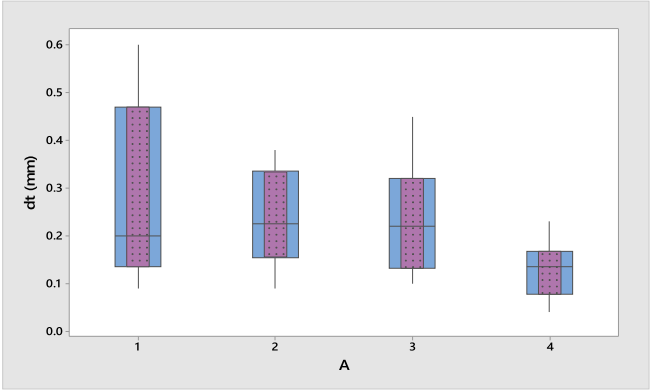

B.

Fig. 4. The dt dataset for factor-settings of A (Table 1): Normal probability plot with 95% confidence interval (A), and boxplots (B).

portion of the data points cannot even be contained within the 95% confidence interval. The indication of non-normality is an inference that is also supported by the result of the Anderson-Darling test ($p < 0.05$) on the same plot. To expose further the data asymmetry, we use a boxplot depiction (Fig. 3B). The strong presence of skewness now becomes more pronounced. It becomes evident that a grand mean estimation would not be meaningful under such severe skewness. This would impair any regular Taguchi-type optimization predictions since the optimal response is dependent on the accuracy of the estimation of the grand mean. Deeper probing, by drilling down through data-screening in terms of factor-settings, reveals the following:

i) *Factor-A*: Setting-A1 data do not obey normality ($p < 0.05$) according to the Anderson-Darling test (Fig. 4A). There is great variation in spreads among boxplots for different settings (Fig. 4B) as well as exaggerated asymmetry, especially for setting A1.
ii) *Factor-B*: Data for settings B2 and B3 do not obey normality ($p < 0.05$) according to the Anderson-Darling test (Fig. 5A). There is great variation of spreads among boxplots for different settings (Fig. 5B) as well as exaggerated asymmetry with respect to settings B2, B3 and B4.
iii) *Factor-C*: All settings appear to obey normality ($p > 0.05$) according to the Anderson-Darling test (Fig. 6A). There is great spread variation among boxplots for different settings (Fig. 6B) as well as skewness for the data related to setting C2.
iv) *Factor*-D: Setting-D1 data do not obey normality ($p < 0.05$) according to the Anderson-Darling test (Fig. 7A). There is great spread variation among boxplots for different settings (Fig. 7B). Data for Setting-D1 are skewed while there are also three outlier/extremity points.

Next, to check the level of repeatability in the collected dataset, we cross-correlate the three-replicate data-vectors (dt1-dt3) through pair-wise line-fitting. The three-resulting linear-regression plots, which are assorted with their respective 95% confidence intervals, are portrayed for the three replicate vectors (Table 1) in Fig. 8. In a nutshell, we observe that the regression fittings are weak. The three corresponding (adjusted) coefficients of determination range from a minimum of 35.2% to a maximum of 78.3%. All regression coefficients fluctuate with a persistent deflection well below unity – from 0.75 to 0.70 ($p < 0.05$). Furthermore, in all three plots of Fig. 8, a significant number of observations pose as outliers; they are situated outside the 95% confidence bands. This is a low confidence signal in a repeatability assessment. An alternative approach might be to check for normality the sixteen individual triads of observations (Table 1); it is clearly not meaningful for replicates of size $n = 3$. The above screening results seem to advocate toward a statistical landscape that suits up for a 'messy' data analysis. At this stage, it becomes evident that a deployed multi-factorial optimization solver should be apt to proceed with the profiling process in the absence of an identified parametric data-distribution.

3.2. Nonparametric multifactorial profiling

By employing the proposed methodology to the dataset of Table 1, first, we rank-order in a single rollout all the replicate vectors (Table 2). Next, we sum-up the ranked replicates for each recipe individually in the same table. In Table 3, we tabulate the effect median estimations. From a visual inspection, it appears that the effects A, B and C might be

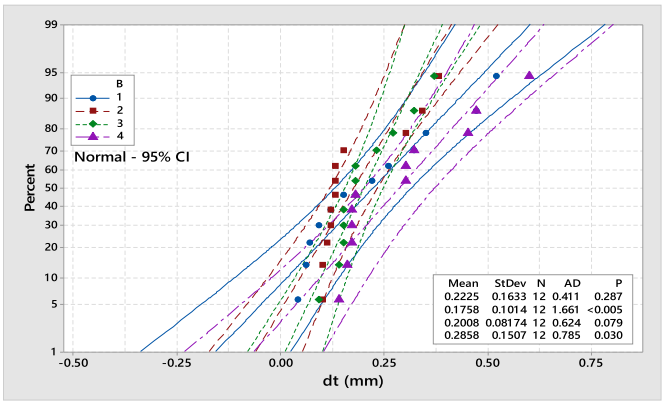

A.

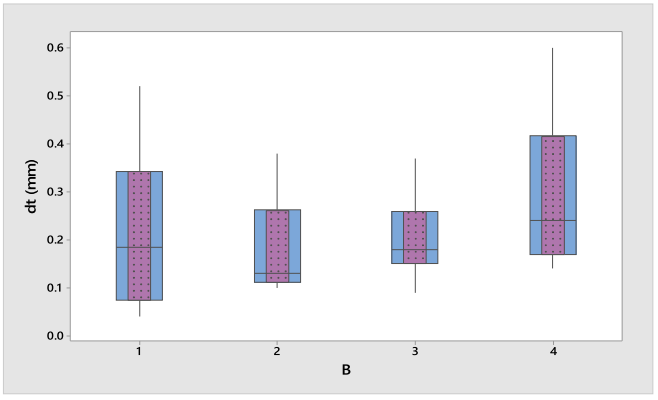

B.

Fig. 5. The dt dataset for factor-settings of B (Table 1): Normal probability plot with 95% confidence interval (A), and boxplots (B).

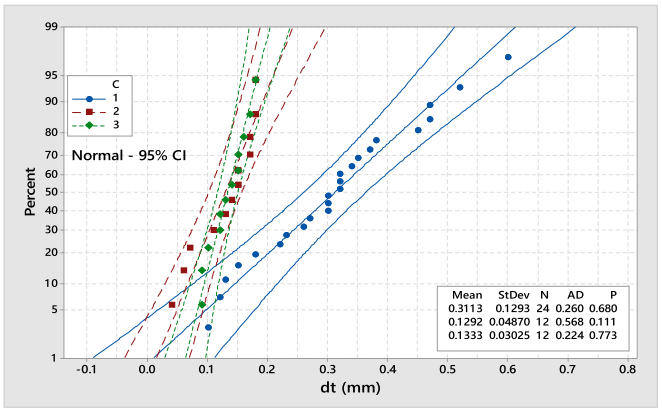

A.

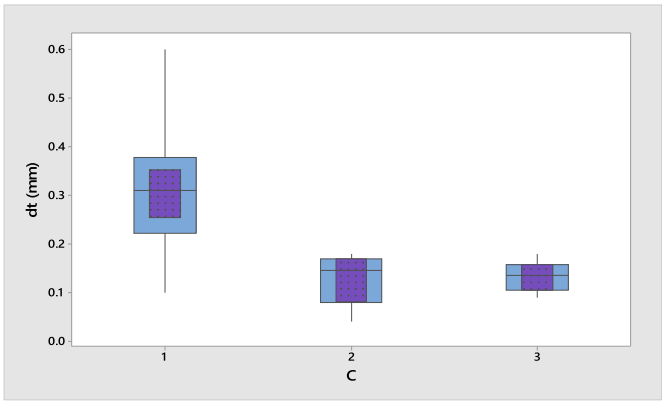

B.

Fig. 6. The dt dataset for factor-settings of C (Table 1): Normal probability plot with 95% confidence interval (A), and boxplots (B).

influential given that the differences of their median rank-sum magnitudes post noticeable variations - from 73 (C-effect) to 48.8 (A-effect). The D-effect is definitely weak. In Table 4, we tabulate the outcomes of the two-stage profiling analysis - the four examined effects and their uncertainties. First, we examine the statistical significance of the uncertainty symmetry within effects. No effect is influenced by an unbalanced load of uncertainty across settings. In all error screenings, we consistently observe that $p > 0.05$. This indicates that we may move on contemplating the outcomes of the strength profiling for all four effects. At a first glance, it is the effects A and C that appear statistically significant at a level of 0.05. However, applying the Benjamini-Hochberg rule (Benjamini and Hochberg, 1995) for controlling the false discovery rate at $\alpha = 0.05$, we conclude that only the C-effect is the only statistically dominant influence. This is because at a controlling false discovery rate of $q^* = \alpha = 0.05$ (Benjamini and Hochberg, 1995), it is only the p-value (p_C) for the C-effect, $p_C = 0.005$ (Table 4), that is less than the critical value of 0.013 ($=\alpha/4$). From Table 3, we note that it is setting C3 that minimizes the median rank-sum response. This setting corresponds to a fan speed of 100%. The significance of this result should be further elucidated in Fig. 9 - in terms of a boxplot screening of the three candidate settings. The corresponding median estimations of the dt values for fan speed levels of 50% and 100% are 0.145 mm and 0.135 mm, respectively. However, we observe that the 95% confidence intervals of the *rs* medians of the two competing settings overlap (Fig. 9).

From a practical perspective then, we select a 50% fan speed in the optimal design. This is because it would simultaneously minimize energy consumption; it is a 'lean' and 'green' solution. This setting solution agrees with the original published solution for the fan speed, which was recommended for the general 'inclined strut' structure case (Dong et al., 2018). Effects A, B and D are judged as inactive. Thus, they may be adjusted to any setting that conveniently or practically benefits the 3D-printing process performance. This may be interpreted as follows:

a) The nozzle temperature (A-effect) should be set to 225 °C. This decision leads to minimizing energy consumption.
b) The print speed (B-effect) should be set to 2400 m/s. This is justified from an optimal 3D-printing performance (maximum production rate).
c) The layer height (D-effect) should be set to 0.2 mm. This is justified from an optimal 3D-printing performance (maximum material deposition).

The solution for the setting adjustments that we recommended above differs in the three out of the four examined 3D-printing parameters. Of course, the comparison concerns the general 'inclined-strut' lattice-structure (published) prediction (Dong et al., 2018). We found that the 'inclined-60°' geometry case, using the failure method of 'max deviation' (Dong et al., 2018), may not be serviced by a general recommendation. The reasons are obvious now. Discrepancies are attributed to the exclusion of the following elements from the published analysis: 1) the non-normality of the dt response, 2) the classical Taguchi method does not allow screening concurrently mean and SNR tendencies, 3) no separation of screening/optimization outcomes, 4) no statistical significance evaluation, and 5) no controlling for false-discovery. From an 'agile production' point of view, the 3D-printing process could be sped-up twice as fast as from it was originally recommended. Finally, the layered ABS-material could be deposited at a double rate with respect to the original thickness specification - according to the published dataset (Dong et al., 2018).

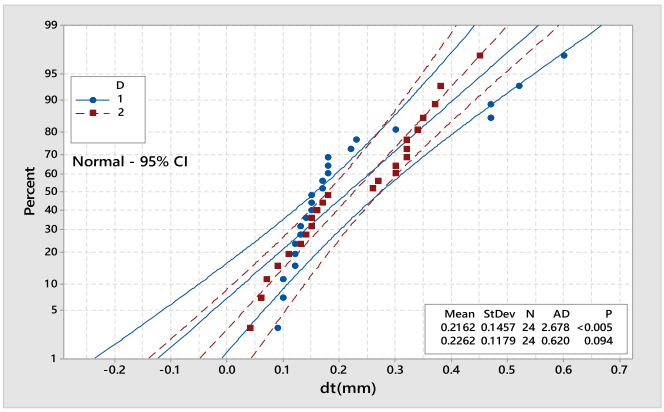

A.

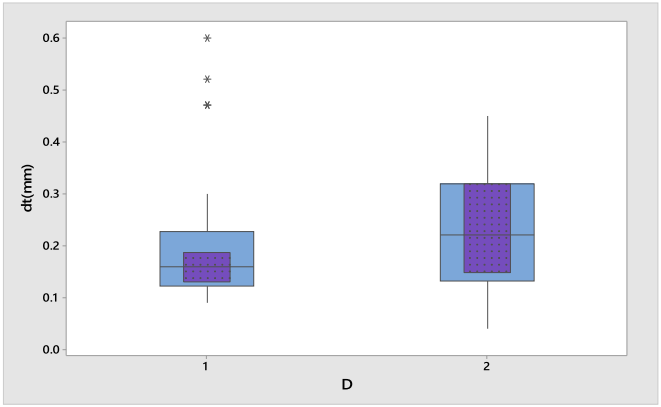

B.

Fig. 7. The dt dataset for factor-settings of D (Table 1): Normal probability plot with 95% confidence interval (A), and boxplots (B).

4. Discussion

We discuss now possible causes for the discrepancies that have emerged from the competing optimization scenarios. The characteristic that was sought to be optimized in the fused deposition case study (Dong et al., 2018) was the difference between the maximum and minimum strut diameter, *dt*. By design, the *dt*-variable should be minimized for improved quality performance. The classical Taguchi-performance measure that was used in the case study (Dong et al., 2018) was the SNR expression that corresponds to a 'smaller-is-better' response (Taguchi et al., 2000, 2004), η (dB). It is defined as follows for a number of n replicates:

$$\eta = -10\, log_{10}\left\{\frac{1}{n}\sum_{i=1}^{n} dt_i^2\right\} \tag{19}$$

However, the averaged sum of the squared differences, in equation (19), may be split in terms of its location (mean, $\overline{dt}$) and dispersion (variance, s^2) components:

$$\frac{1}{n}\sum_{i=1}^{n} dt_i^2 = \left(\overline{dt}\right)^2 + \frac{n-1}{n}s^2 \quad \text{with} \quad \overline{dt} = \frac{1}{n}\sum_{1}^{n} dt_i$$

$$\text{and} \quad s^2 = \frac{1}{n-1}\sum_{1}^{n}\left(dt_i - \overline{dt}\right)^2 \tag{20}$$

As long as the respective magnitudes of the squared mean and the variance estimations of the *dt* variable are of the same order in the SNR expression, they may be regarded useful in extracting information. Otherwise, the squared mean and the variance estimations may be confounded rendering the screening/optimization result misleading (Logothetis, 1990). This condition causes major concern because if the two measuring scales are not comparable, it may lead to biased outcomes and eventually spurious (suboptimal) solutions. To examine the relative behavior of the two estimators for the strut-diameter range variable, the mean and standard deviation (s) of the replicated dataset (Table 1) are

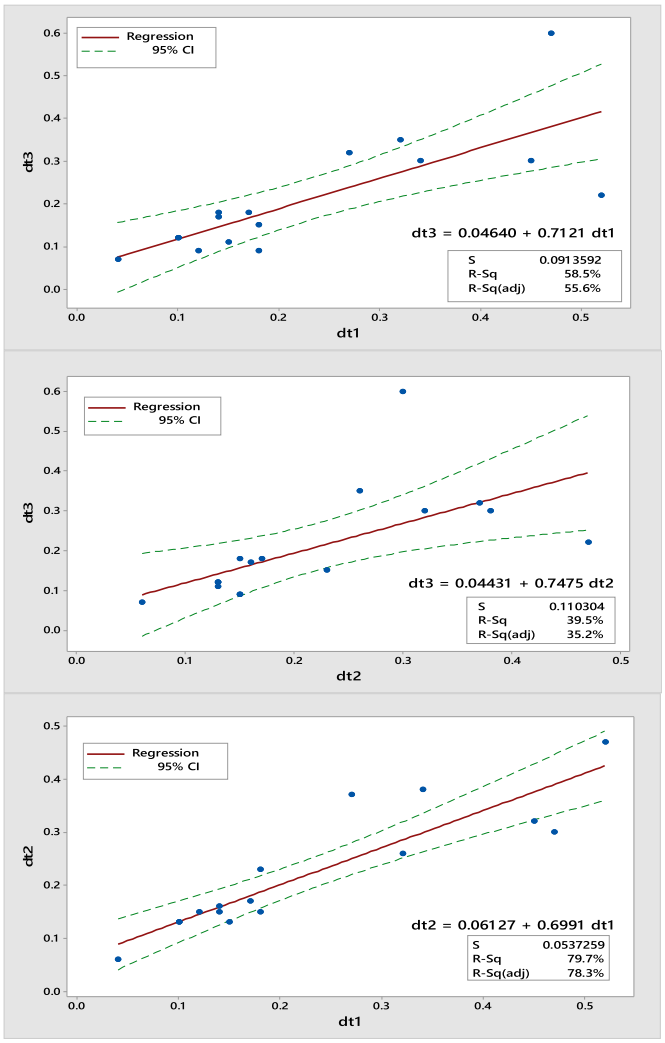

Fig. 8. Line fittings between pairs of replicate data (Table 1): Top: dt3 vs dt1, middle: dt3 vs dt2, bottom: dt2 vs dt1.

Table 2
The rank-ordered and rank-summed conversion of the dataset of Table 1.

Run #	r1	r2	r3	Rs
1	47	45	30	122
2	19	12.5	8	39.5
3	27	19	4.5	50.5
4	46	35.5	48	129.5
5	10	19	4.5	33.5
6	40	43	34	117
7	33	42	38.5	113.5
8	24	24	27	75
9	38.5	32	41	111.5
10	6.5	14	10	30.5
11	15	19	27	61
12	44	37	35.5	116.5
13	1	2	3	6
14	6.5	12.5	10	29
15	29	31	19	79
16	16	22	24	62

Table 3
Nonparametric response table for the four effects of the fused deposition.

Factor	Setting	Median rs
A	1	86.3
	2	94.3
	3	86.3
	4	45.5
B	1	72.5
	2	35.0
	3	70.0
	4	95.8
C	1	115.0
	2	50.3
	3	42.0
D	1	68.0
	2	86.8
Grand Median		68.5

Table 4
Nonparametric profiling of the four effects and their uncertainty balance.

Factor	Uncertainty balance	P	Effect strength	P
	U/H[a]		U/H[a]	
A	6.64	0.084	8.74	0.033
B	2.54	0.469	4.52	0.21
C	1.61	0.447	10.61	0.005
D	24.00	0.442	27.00	0.645

[a] U-estimator for Wilcoxon-Mann-Whitney test, H-estimator for Kruskal-Wallis test.

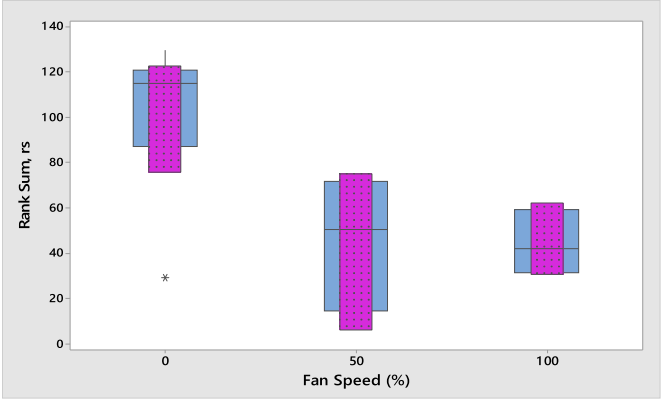

Fig. 9. Boxplot comparisons of rank-sum response (*rs* variable) for the three settings of the fan speed factor.

Table 5
Range means and standard deviation for the dataset of Table 1.

run #	$\overline{dt}$	S	$\overline{dt}/s$
1	0.403	0.161	2.5
2	0.130	0.020	6.5
3	0.140	0.046	3.1
4	0.457	0.150	3.0
5	0.120	0.030	4.0
6	0.340	0.040	8.5
7	0.320	0.050	6.4
8	0.173	0.006	30.0
9	0.310	0.046	6.8
10	0.117	0.015	7.6
11	0.157	0.021	7.5
12	0.357	0.081	4.4
13	0.057	0.015	3.7
14	0.117	0.015	7.6
15	0.187	0.040	4.6
16	0.157	0.015	10.3

tabulated in Table 5. The ratio of the strut-diameter-range mean over the strut-diameter-range standard deviation reveals that there is a significant difference in the magnitudes of the two scales. For the sixteen calculated entries in the experimental design, their average ratio value is 7.3. Thus, using exclusively η as a robust performance measure might potentially lead to a biased result. To proceed with the analysis, we ought to explore whether there exists a relationship between the mean and the standard deviation variables. The customary approach to accomplish this is to fit an appropriate function using the Box-Cox transformation (Logothetis, 1990). The mean and standard deviation estimations, from the strut-diameter range dataset of Table 5, are firstly log-transformed and, next, they are line-fitted according to the equation (Logothetis, 1990):

$$log_{10}(s_i) = a + b \times log_{10}\left(\overline{dt}_i\right) + \varepsilon_i\ ,\ i = 1,\ 2,\ \ldots,\ n \tag{21}$$

In Fig. 10, we observe that the performed line-fitting effort is rather unsuccessful, because the (adjusted) coefficient of determination is low enough (52.3%) to offer some insight.

Moreover, there are several data points that defy the boundaries which are set by the estimated 95% confidence interval. Hence, the regression analysis results also attest to a 'messy outlook'. We may contemplate that a transformation for the strut-diameter-range dataset may be dubious to pursue at this point. It may be implied that a functional relationship between the mean and the standard-deviation estimators might not even exist. Even so, the urgent task is to prevent the imminent confounding owing to the dominating influence of the mean values over the SNR estimations. Consequently, we should seek for suitable performance measures that allow the decoupling of the two contributions – the mean and standard deviation. Obviously, two separate steps are required to identify the factor settings that control: 1) the 'signal' (mean) and 2) the 'noise' (variance). The two recommended expressions for the proper signal measure (*SM*) and the noise measure (*NM*) respectively are (Logothetis, 1990):

$$SM = \overline{dt}_i \quad \text{and} \quad NM = -10log_{10}\left(s_i^2\right) \tag{22}$$

We graph the main-effects plots for the strut-diameter-range *SM* variable (Fig. 11 A) and the strut-diameter-range *NM* variable (Fig. 11B). From a visual inspection, we observe that effects A and C may be susceptible to factorial adjustment because they generate similar variation. Sieving through the dataset using the ANOVA treatment (Tables 6 and 7), we identify the A-effect and C-effect as the only two posing as statistically significant at a level of 0.05. However, controlling the false discovery rate at $q^* = \alpha = 0.05$ (Benjamini and Hochberg, 1995), it is only the p-value (p_C) for the C-effect ($p_C = 0.002$ (Table 6), $p_C = 0.006$ (Table 7)) that is consistently smaller than the critical value of 0.013 ($=\alpha/4$). The p-values for the strut-diameter-range means (Table 6) and strut-diameter-range noise dispersion (Table 7) are of the same low order (highly significant). Still, this screening solution agrees in its entirety with our proposed solution and partly disagrees with the original findings; the published solution concluded that all four factors were strong (Dong et al., 2018). Minimizing the *SM* variable (Fig. 11A) and maximizing the *NM* variable (Fig. 11B) converge on optimizing the fan speed behavior at the setting of 50% (setting C2).

The same practical outcome is also gleaned from the separate boxplot depictions of the two sets of measures (Fig. 12). In congruence to the logic in our proposed optimization-method prescription, the median values for the strut-diameter-range *SM* variable (Fig. 12 A) and strut-diameter-range *NM* variable (Fig. 12 B) are statistically of indistinguishable strength at their respective settings of 50% (C2) and 100% (C3). Consequently, from practical considerations, the fan speed would be optimally adjusted at the 50% setting by simultaneously incorporating information from both *SM* and *NM* responses. The remaining three (statistically weak) factors should receive an adjustment that best aligns to matters of practicality, cost and/or convenience. Justifiably, then, the solution in this case is merely a parallel narration of our proposed

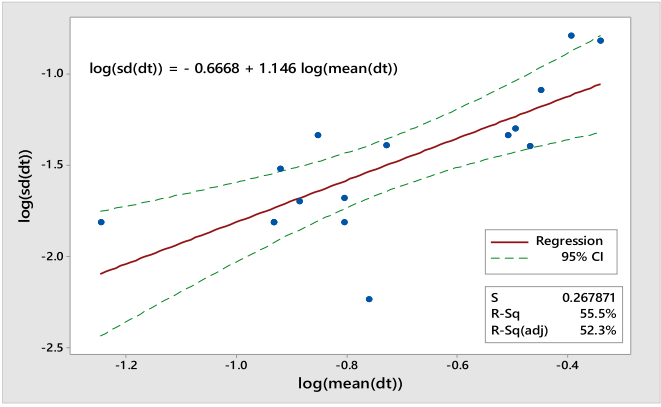

Fig. 10. Fitting the log-transformed values of the standard deviation against the mean (for the strut diameter range dataset of Table 5).

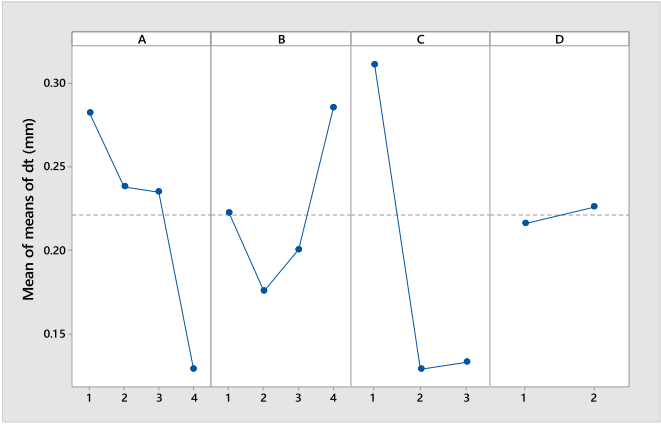

A.

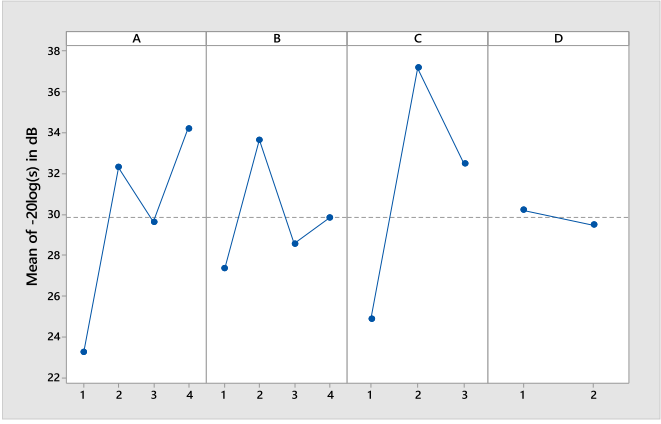

B.

Fig. 11. Main-effect plots for range data: A) means ($\overline{dt_i}$) and B) noise dispersion ($-10log_{10}(s_i^2)$).

solution in the preceding section.

In comparison to the alternative treatment and the discussed complications arising from using the SNR transformation in multifactorial screening/optimization problems, it is evident that our technique: 1) reaches to optimal solution in a single screening/optimization pass (combo-solution 'two-in-one'), 2) there is no need to separate to location and dispersion components for the replicates, and 3) all required statistical quantities are primed to sustain solution robustness.

The solver robustness as well as the convenience of no-decoupling of

Table 6
Analysis of variance for range means ($\overline{dt_i}$).

Factor[a]	DF	SS	MS	F	P
A	3	0.050847	0.016949	5.94	0.032
B	3	0.026608	0.008869	3.11	0.110
C	2	0.129635	0.064817	22.70	0.002
D	1	0.000400	0.000400	0.14	0.721
Residual Error	6	0.017129	0.002855		
Total	15	0.224619			

[a] R^2 (adjusted) = 80.9%.

Table 7
Analysis of variance for range noise dispersion ($-10log_{10}(s_i^2)$).

Factor[a]	DF	SS	MS	F	P
A	3	273.279	91.093	5.53	0.037
B	3	88.934	29.645	1.80	0.247
C	2	439.504	219.752	13.34	0.006
D	1	2.076	2.076	0.13	0.735
Residual Error	6	98.854	16.476		
Total	15	902.648			

[a] R^2 (adjusted) = 72.6%.

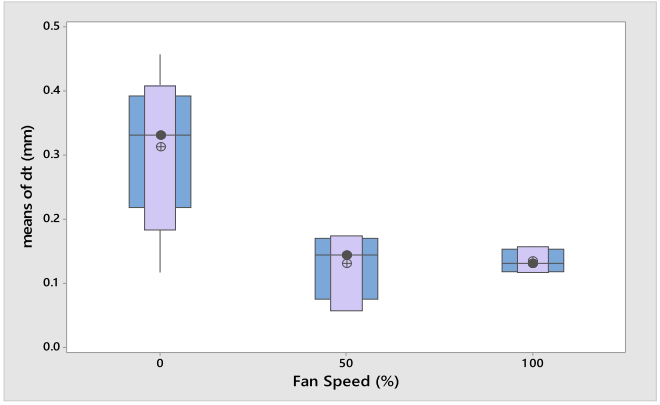

A.

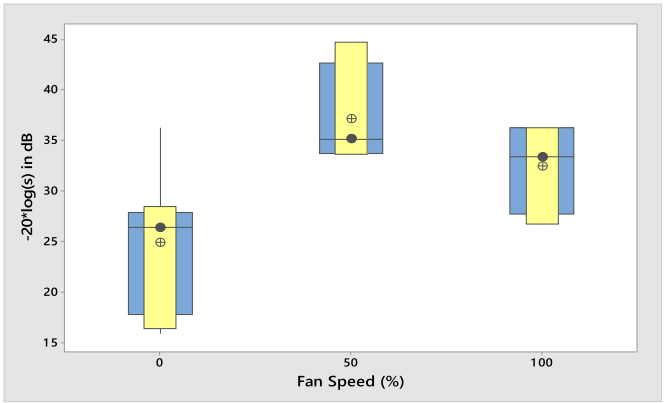

B.

Fig. 12. Box plots of fan speed for: A) range means ($\overline{dt_i}$), and B) range noise dispersion ($-10log_{10}(s_i^2)$).

the estimators in terms of location and dispersion components is clearly attributed to the innate statistical framework of classical non-parametrics. The proposed optimization routine managed to incorporate in its inner workings both of those critical features, thus taking maximum advantage of the complementary permutation theory of Wilcoxon and Mann-Whitney. It is this facility that permits the direct

comparison between samples ('micro-populations') that may have been gathered from various - sometimes even unknowable - distributions. Relying on this advantage makes our proposed profiling more lean (less and faster work) and more agile (applicable everywhere). Although, this thinking is an indispensable part for any modern improvement procedure, it might also be beneficial to highly complex 3D-printing processes.

The proposed methodology aspires to be simple (lean), responsive (agile) and resilient (robust) by design. These characteristics are paramount in additive manufacturing due to the lack of: 1) a single physical model that comprehensively describes the 3D-printing phenomena, and 2) a single established data analyzer to quantify the accompanying process uncertainties. Our proposal attempts to reshape the instrument that measures the cause-and-effect relationship in the traditional DOE/Taguchi approach. By heeding to risky events that might loom in the investigated stochastic landscape, it offers a rudimentary protection against an otherwise undermined result; an occurrence which is perhaps associated with counting on a mere naïve application of ordinary alternatives (data-analytic). Inexorably, outcomes that have been generated from FFD-based DOE treatments might occasionally become dicey, because the small data condition – inherently ingrained in the parsimonious philosophy of the Taguchi-type collection scheme - might harbor several opportunities that would tend to steer a DOE study to a fallacious diagnosis. The real circumstances that could give rise to such possibilities are:

1) The smallness of the replicates renders a classical solver vulnerable against the detrimental effects of the two familiar contingencies: a) normal data to behave as departing from normality and 2) non-normal data to appear behaving as normal.
2) The necessity to evaluate replicate information from both - location and dispersion - perspectives at the same time (in a single action).
3) The necessity to evaluate information from location and dispersion measures at the same time (in a single action) for all factor levels - irrespectively of the mix, type and number of the factor levels in the experimental scheme.
4) The desire for a solver that it transpires to be computationally simple ("terse and swift") - on par with the sparing data collection tactics.

To respond to the above concerns, it is obvious that the pure nonparametric framework of the solver automatically remedies the first predicament. Nonparametrics are impervious to any prior dataset fingerprinting. The second and third concerns are alleviated because the Wilcoxon/Mann-Whitney statistics zoom out to encircle information from the broader distribution propensities (Mann and Whitney, 1947). The fourth item has been resolved by virtue of the preset reference law in the Wilcoxon/Mann-Whitney statistics and its unlimited adaptability to messy datasets (Scheffe and Tukey, 1945; Draper, 1988).

5. Conclusion

We proposed a robust multifactorial screening/optimization method that exploits scarce information from OA-generated data schemes in order to facilitate the amelioration of 3D-printing process characteristics. The statistical profiler capability was directly exemplified on mixed-scheme Taguchi-type orthogonal datasets that were collected from fabricating lattice structures by a fused deposition process. The showcased paradigm was intriguing because it offered the opportunity to concurrently manipulate inherent material and geometrical complexities - a daunting task in additive manufacturing. Thus, ample emphasis was placed on illustrating that natural 'data messiness' lurking in interpreting 3D-printing process variables. Several statistical complications were spotlighted in association to data non-normality, heteroscedasticity, robustness and convertibility. Particularly, we elaborated on the perplexing phenomenon of data conversion using a classical Taguchi-type SNR-performance measure. It was shown that data reduction using an SNR estimator might not always be robust and could lead to misdiagnosing those critical 3D-printing effects that need careful tuning. The robustness of optimal predictions hinged upon the de-confounding of the signal and the noise that represented the collected 3D-printing dataset.

The proposed method was shown to circumvent this problem by introducing well-accepted distribution-free estimators for replicating small samples. Our solution is in accord with the solution of an older DOE approach that demanded the decoupling of the signal and the noise. Key advantage of our proposal is that it reaches to a prediction in half the effort since the older DOE method requires screening the dataset twice for effect strength. Both commented approaches are in agreement with the identification of just a single effect (fan speed) as well as its optimal adjustment (50%). This is also in agreement with the published solution. However, in search of minimizing the range of the strut diameter in the paradigm, both discussed predictions affirmed that the remaining effects appear weak, in disagreement with the original predictions. Further suggestions for future work could include projects that consider the concurrent optimization of multiple 3D-printing characteristics, larger group of examined effects and the influence of partial interactions among effects.

Acknowledgements

We thank the Editor in Chief and the reviewers for their critical comments that led to the improvement of this work.

References

Afshari, H., Searcy, C., Jaber, M.Y., 2020. The role of eco-innovation drivers in promoting additive manufacturing in supply chains. Int. J. Prod. Econ. 223, 107538.
Alves, A.C., Dinis-Carvalho, J., Sousa, R.M., 2012. Lean production as promoter of thinkers to achieve companies' agility. Learn. Organ. 19, 219–237.
Attaran, M., 2017. The rise of the 3-D printing: the advantages of additive manufacturing over traditional manufacturing. Bus. Horiz. 60, 677–688.
Bandyopadhyay, A., Heer, B., 2018. Additive manufacturing of multi-material structures. Mater. Sci. Eng. R 129, 1–16.
Benjamini, Y., Hochberg, Y., 1995. Controlling the false discovery rate: a practical and powerful approach to multiple testing. J. Roy. Stat. Soc. 57, 289–300.
Besseris, G.J., 2013. A distribution-free multi-factorial profiler for harvesting information from high-density screenings. PloS One 8, e73275.
Besseris, G.J., 2014. A fast-and-robust profiler for improving polymerase chain reaction diagnostics. PloS One 9, e108973.
Bhamu, J., Sangwan, K.S., 2014. Lean manufacturing: literature review and research issues. Int. J. Prod. Qual. Manag. 34, 876–940.
Bose, S., Ke, D., Sahasrabudhe, H., Bandyopadhyay, A., 2018. Additive manufacturing of biomaterials. Prog. Mater. Sci. 93, 45–111.
Box, G.E.P., 1988. Signal-to-noise ratios, performance criteria and transformation. Technometrics 30, 1–17.
Box, G.E.P., Hunter, W.G., Hunter, J.S., 2005. Statistics for Experimenters – Design, Innovation, and Discovery, second ed. Wiley, New York.
Briggs, W., 2016. Uncertainty: the Soul of Modeling, Probability and Statistics, first ed. Springer International, Switzerland.
Carlson, J.M., Doyle, J., 2002. Complexity and robustness. Proc. Natl. Acad. Sci. Unit. States Am. 99, 2538–2545.
Chang, J., He, J., Mao, M., Zhou, W., Lei, Q., Li, X., Li, D., Chua, C.-K., Zhao, X., 2018. Advanced material strategies for next-generation additive manufacturing. Materials 11, 166.
Chua, C.K., Leong, K.F., 2017. 3D Printing and Additive Manufacturing, fifth ed. World Scientific Publishing.
Colosimo, B.M., Huang, Q., Dasgupta, T., Tsung, F., 2018. Opportunities and challenges of quality engineering for additive manufacturing. J. Qual. Technol. 50, 233–252.
Crosby, P.B., 1979. Quality Is Free: the Art of Making Quality Certain, first ed. McGraw-Hill.
Cuellar, J.S., Smit, G., Plettenburg, D., Zadpoor, A., 2018. Additive manufacturing of non-assembly mechanisms. Addit. Manuf. 21, 150–158.
Cunningham, C.R., Flynn, J.M., Shokrani, A., Dhokia, V., Newman, S.T., 2018. Strategies and processes for high quality wire arc additive manufacturing. Addit. Manuf. 22, 672–686.
Dastjerdi, A.A., Movahhedy, M.R., Akbari, J., 2017. Optimization of process parameters for reducing warpage in selected laser sintering of polymer parts. Addit. Manuf. 18, 285–294.
Dizon, J.R.C., Espera Jr., A.H., Chen, Q., Advincula, R.C., 2018. Mechanical characterization of 3D-printed polymers. Addit. Manuf. 20, 44–67.
Dong, G., Wijaya, G., Tang, Y., Zhao, Y.F., 2018. Optimizing process parameters of fused deposition modeling by Taguchi method for the fabrication of lattice structures. Addit. Manuf. 19, 62–72.

Draper, D., 1988. Rank-based robust analysis of linear models, Part 1: exposition and review. Stat. Sci. 3, 239–257.
Eyers, D.R., Potter, A.T., 2017. Industrial Additive Manufacturing: a manufacturing systems perspective. Comput. Ind. 92–93, 208–218.
Farahani, R.D., Dube, M., 2018. Printing polymer nanocomposites and composites in three dimensions. Adv. Eng. Mater. 20, 1700539.
Fera, M., Macchiaroli, R., Fruggiero, F., Lambiase, A., 2018. A new perspective for production process analysis using additive manufacturing—complexity vs production volume. Int. J. Adv. Manuf. Technol. 95, 673–685.
Fitzharris, E.R., Watt, I., Rosen, D.W., Shofner, M.L., 2018. Interlayer bonding improvement of material extrusion parts with polyphenylene sulfide using the Taguchi method. Addit. Manuf. 24, 287–297.
Francois, M.M., Sun, A., King, W.E., Henson, N.J., Tourret, D., Bronkhorst, C.A., Carlson, N.N., Newman, C.K., Haut, T., Bakosi, J., Gibbs, J.W., Livescu, V., Van der Wiel, S.A., Clarke, A.J., Schraad, M.W., Blacker, T., Lim, H., Rodgers, T., Owen, S., Abdeljawad, F., Madison, J., Anderson, A.T., Fattebert, J.-L., Ferencz, R.M., Hodge, N.E., Khairallah, S.A., Walton, O., 2017. Modeling of additive manufacturing processes for metals: challenges and opportunities. Curr. Opin. Solid State Mater. Sci. 21, 198–206.
Fundin, A., Bergquist, B., Eriksson, H., Gremyr, I., 2018. Challenges and propositions for research in quality management. Int. J. Prod. Econ. 199, 125–137.
Ganeshan, R., Kulkarni, S., Boone, T., 2001. Production economics and process quality: a Taguchi perspective. Int. J. Prod. Econ. 71, 343–350.
Gao, W., Zhang, Y.B., Ramanujan, D., Ramani, K., Chen, Y., Williams, C.B., Wang, C.C.L., Shin, Y.C., Zhang, S., Zavattieri, P.D., 2015. The status, challenges, and future of additive manufacturing in engineering. Comput. Aided Des. 69, 65–89.
Garg, A., Tai, K., Savalani, M.M., 2014. State-of-the-art in empirical modelling of rapid prototyping processes. Rapid Prototyp. J. 20, 164–178.
George, M.L., Maxey, J., Rowlands, D., Price, M., 2004. The Lean Six Sigma Pocket Toolbook: A Quick Reference Guide to 100 Tools for Improving Quality and Speed, first ed. McGraw-Hill.
Ghobadian, A., Talavera, I., Bhattacharya, A., Kumar, V., Garza-Reyes, J.A., O'Regan, N., 2020. Examining legitimatisation of additive manufacturing in the interplay between innovation, lean manufacturing and sustainability. Int. J. Prod. Econ. 219, 457–468.
Gholaminezhad, I., Assimi, H., Jamali, A., Vajari, D.A., 2016. Uncertainty quantification and robust modeling of selective laser melting process using statistical multi-objective approach. Int. J. Adv. Manuf. Technol. 86, 1425–1441.
Gibson, I., Rosen, D.W., Stucker, B., 2015. Additive Manufacturing Technologies: 3D Printing, Rapid Prototyping, and Direct Digital Manufacturing, second ed. Springer.
Goh, T.N., 1992. An organizational approach to product quality via statistical experiment design. Int. J. Prod. Econ. 27, 167–173.
Hettmansperger, T.P., McKean, J.W., 2010. Robust Nonparametric Statistical Methods, second ed. CRC Press.
Hoaglin, D.C., Mosteller, F., Tukey, J.W., 2000. Understanding Robust and Exploratory Data Analysis. Wiley-Interscience, Hoboken, NJ.
Hollander, M., Wolfe, D.A., Chicken, E., 2013. Nonparametric Statistical Methods, third ed. Wiley.
Huber, P.J., Ronchetti, E.M., 2009. Robust Statistics. Wiley, Hoboken, NJ.
Kacarevic, Ž.P., Rider, P.M., Alkildani, S., Retnasingh, S., Smeets, R., Jung, O., Ivanišević, Z., Barbeck, M., 2018. An introduction to 3D bioprinting: possibilities, challenges and future aspects. Materials 11, 2199.
Kim, H., Lin, Y., Tseng, T.-L.B., 2018. A review on quality control in additive manufacturing. Rapid Prototyp. J. 24, 645–669.
Kovach, J., Stringfellow, P., Turner, J., Cho, B.R., 2005. The house of competitiveness: the marriage of agile manufacturing, design for six sigma, and lean manufacturing with quality considerations. J. Ind. Technol. 21, 1–10.
Kruskal, W.H., Wallis, W.A., 1952. Use of ranks in one-criterion variance analysis. J. Am. Stat. Assoc. 47, 583–621.
Kuhn, M., Schaefer, F., Otten, H., 2018. Process complexity as a future challenge-a quality management perspective. TQM J 30, 701–716.
Le, M., 2018. May, Agile for Everybody: Creating Fast, Flexible, and Customer-First Organizations, first ed. O' Reilly Media.
Lee, J.-Y., An, J., Chua, C.K., 2017. Fundamentals and applications of 3D printing for novel materials. Applied Materials Today 7, 120–133.
Lipson, H., Kurman, M., 2013. Fabricated: the New World of 3D Printing. Wiley.
Logothetis, N., 1990. Box-Cox transformations and the Taguchi method. Appl. Stat. 39, 31–48.
Loh, G.H., Pei, E., Harrison, D., Monzón, M.D., 2018. An overview of functionally graded additive manufacturing. Addit. Manuf. 23, 34–44.
Ludbrook, J., Dudley, H., 1998. Why permutation tests are superior to *t* and *F* tests in biomedical research. Am. Statistician 52, 127–132.
Maghsoodloo, S., Ozdemir, G., Jordan, V., Huang, C.-H., 2004. Strengths and limitations of Taguchi's contributions to quality, manufacturing, and process engineering. J. Manuf. Syst. 23, 73–126.
Mahmooda, S., Qureshib, A.J., Talamona, D., 2018. Taguchi based process optimization for dimension and tolerance control for fused deposition modelling. Addit. Manuf. 21, 183–190.
Mann, H.B., Whitney, D.R., 1947. On a test of whether one of two random variables is statistically larger than the other. Ann. Math. Stat. 18, 50–60.
Mellor, S., Hao, L., Zhang, D., 2014. Additive manufacturing: a framework for implementation. Int. J. Prod. Econ. 149, 194–201.
Milliken, G.A., Johnson, D.E., 1989. Analysis of Messy Data, vol. II. Nonreplicated Experiments. Chapman and Hall/CRC, Boca Raton.
Milliken, G.A., Johnson, D.E., 2004. Analysis of Messy Data, vol I. Designed Experiments, Chapman and Hall/CRC, Boca Raton.
Murthy, D.N.P., Ravi Kumar, K., 2000. Total product quality. Int. J. Prod. Econ. 67, 253–267.
Natarajan, R., 1993. Determining input parameters under process uncertainties. Int. J. Prod. Econ. 29, 203–210.
Ngo, T.D., Kashani, A., Imbalzano, G., Nguyen, K.T.Q., Hui, D., 2018. Additive manufacturing (3D printing): a review of materials, methods, applications and challenges. Composites B 143, 172–196.
Oh, Y., Zhou, C., Behdad, S., 2018. Part decomposition and assembly-based (Re) design for additive manufacturing: a review. Addit. Manuf. 22, 230–242.
Orr, H.A., 2000. Adaptation and the cost of complexity. Evolution 54, 13–20.
Parandoush, P., Lin, D., 2017. A review on additive manufacturing of polymer-fiber composites. Composites Stuctures 182, 36–53.
Petrick, I.J., Simpson, T.W., 2013. 3D printing disrupts manufacturing. Res. Technol. Manag. 56 (6), 12–16.
Pett, M.A., 2015. Nonparametric Statistics for Health Care Research: Statistics for Small Samples and Unusual Distributions, second ed. SAGE publications.
Pignatiello, J.J., Ramberg, J.S., 1992. Top ten triumphs and tragedies of Genichi Taguchi. Qual. Eng. 4, 211–225.
Potdar, P.K., Routroy, S., Behera, A., 2017. Agile manufacturing: a systematic review of literature and implications for future research. Benchmark 24, 2022–2048.
Quan, Z., Wu, A., Keefe, M., Qin, X., Yu, J., Suhr, J., Byun, J.-H., Kim, B.-S., Chou, T.-W., 2015. Additive manufacturing of multidirectional preforms for composites: opportunities and challenges. Mater. Today 18, 503–512.
Redwood, B., Schoffer, F., Garret, B., 2017. The 3D Printing Handbook. 3D HUBS.
Satish Prakash, K., Nancharaih, T., V Subba Rao, V., 2018. Additive manufacturing techniques in manufacturing - an overview. Mater. Today: Proceedings 5, 3873–3882.
Scheffe, H., Tukey, J.W., 1945. Non-parametric estimation, Part 1: validation of order statistics. Ann. Math. Stat. 16, 187–192.
Schippers, W.A.J., 1998. Applicability of statistical process control techniques. Int. J. Prod. Econ. 56–57, 525–535.
Siebert, C.F., Siebert, D.C., 2017. Data Analysis with Small Samples and Non-normal Data: Nonparametrics and Other Strategies. Oxford University Press.
Silver, N., 2015. The Signal and the Noise: Why So Many Predictions Fail-But Some Don't, first ed. Penguin, New York.
Taguchi, G., Chowdhury, S., Taguchi, S., 2000. Robust Engineering: Learn How to Boost Quality while Reducing Costs and Time to Market. McGraw-Hill, New York.
Taguchi, G., Chowdhury, S., Wu, Y., 2004. Quality Engineering Handbook. Wiley-Interscience, Hoboken.
Tari, J.J., Sabater, V., 2009. Quality tools and techniques: are they necessary for quality management? Int. J. Prod. Econ. 92, 267–280.
Thomas-Seale, L.E.J., Kirkman-Brown, J.C., Attallah, M.M., Espino, D.M., Shepherd, D.E.T., 2018. The barriers to progression of additive manufacture: perspectives from UK industry. Int. J. Prod. Econ. 198, 104–118.
Thompson, M.K., Moroni, G., Vaneker, T., Fadel, G., Campbell, R.I., Gibson, I., Bernard, A., Schulz, J., Graf, P., Ahuja, B., Martina, F., 2016. Design for additive manufacturing: trends, opportunities, considerations, and constraints. CIRP Ann. - Manuf. Technol. 65, 737–760.
Tofail, S.A.M., Koumoulos, E.P., Bandyopadhyay, A., Bose, S., O'Donoghue, L., Charitidis, C., 2018. Additive manufacturing: scientific and technological challenges, market uptake and opportunities. Mater. Today 21, 22–37.
Trivedi, M., Jee, J., Silva, S., Blomgren, C., Pontinha, V.M., Dixon, D.L., Van Tassel, B., Bortner, M.J., Williams, C., Gilmer, E., Haring, A.P., Halper, J., Johnson, B.N., Kong, Z., S Halquist, M., Rocheleau, P.F., Long, T.E., Roper, T., Wijesinghe, D.S., 2018. Additive manufacturing of pharmaceuticals for precision medicine applications: a review of the promises and perils in implementation. Addit. Manuf. 23, 319–328.
Virmani, N., Saha, R., Sahai, R., 2018. Leagile manufacturing: a review paper. Int. J. Prod. Qual. Manag. 23, 385–421.
Wang, X., Jiang, M., Zhou, Z., Gou, J., Hui, D., 2017. 3D printing of polymer matrix composites: a review and prospective. Composites B 110, 442–458.
Welch, J.J., Waxman, D., 2003. Modularity and the cost of complexity. Evolution 57, 1723–1734.
Wilcoxon, F., 1945. Individual comparisons by ranking methods. Biometrics 1, 80–83.
Wu, H.-C., Chen, T.-C.T., 2018. Quality control issues in 3D-printing manufacturing: a review. Rapid Prototyp. J. 24, 607–614.
Yan, Q., Dong, H., Su, J., Han, J., Song, B., Wei, Q., Shi, Y., 2018. A review of 3D printing technology for medical applications. Engineering 4, 729–742.